Bulletin of the Seismological Society of America, Vol. 103, No. 2B, pp. 1584–1602, May 2013, doi: 10.1785/0120120281

Simultaneous Reactivation of Two, Subparallel, Inland Normal Faults during the M_w 6.6 11 April 2011 Iwaki Earthquake Triggered by the M_w 9.0 Tohoku-oki, Japan, Earthquake

by S. Toda and H. Tsutsumi

Abstract The gigantic M_w 9.0 11 March 2011 Tohoku-oki earthquake suddenly changed the overriding inland area to an extensional stress regime and triggered massive seismic swarms in the coastal region. The largest earthquake of M_w 6.6 struck southern Fukushima on 11 April 2011 and ruptured two previously mapped faults, the northwest (NW)-trending Yunodake fault and the north-northwest (NNW)-trending Itozawa fault. Clear 15-km-long and 14-km-long surface ruptures appeared along both faults, respectively, exhibiting a predominantly normal sense of slip, down to the west. The maximum vertical offset on the Yunodake fault is ~0.8 m, whereas that on the Itozawa fault is ~2.1 m. The Itozawa fault rupture is in part marked by uphill-facing scarps, which is discordant with the large-scale topography but consistent with saddled ridges and ponded alluvium. The Yunodake fault, which bounds a Neogene half-graben structure juxtaposing Mesozoic metamorphic rocks against Neogene sedimentary rocks, shows left-lateral deflections of streams. Seismological data and interviews of local residents revealed that the two subparallel faults ruptured simultaneously. Based on the location of its hypocenter, we, however, interpret that the Itozawa rupture was primary and then triggered normal faulting on the Yunodake fault under the heightened Coulomb stress caused by the preceding Tohoku-oki earthquake. Our paleoseismic trench across the Itozawa fault exposed evidence for a penultimate earthquake that occurred sometime between 12,620 and 17,410 cal yr B.P. There is no evidence that the Itozawa fault ruptured during or immediately after the A.D. 869 Jogan earthquake, which is believed to be the penultimate giant megathrust earthquake along the Japan trench.

Introduction

The 11 March 2011 M 9.0 Tohoku-oki earthquake ruptured a 500-km-long and 200-km-wide megathrust of the interface between the Pacific plate and the overriding Eurasian plate with a maximum displacement of ~50 m (e.g., Simons *et al.*, 2011). The Tohoku-oki earthquake produced a devastating ~20-m-high tsunami (Mori *et al.*, 2011). It also caused a significant eastward movement of the Pacific coast of up to 5.3 m (Ozawa *et al.*, 2011) that changed the inland region from a zone of secular interseismic east–west (EW) contraction to a zone of significant EW stretching. Widespread off-fault aftershocks as far as ~450 km from the locus of high seismic slip (Toda *et al.*, 2011) and their complex fault-plane solutions (Asano *et al.*, 2011; Kato *et al.*, 2011) bear out the extensive coseismic stress change. Large offshore aftershocks caused by normal faulting explicitly demonstrate extraordinary stress perturbation, possibly suggesting a more than ~30° rotation of the principal stress axes (Hasegawa *et al.*, 2011).

The highly active normal-faulting aftershocks in part extended westward and onshore, in particular to an area of the southern Fukushima and northern Ibaraki prefectures (hereafter referred to as the Hamadori region; Fig. 1). The unusually high seismicity started immediately after the 11 March M_w 9.0 Tohoku-oki earthquake and has continued for longer than one year (to present) as an extensive massive seismic swarm including 4 $M \geq 6$ and 33 $M \geq 5$ earthquakes in the area shown in Figure 1. The northeast (NE)-trending, 80-km-long, seismic swarm zone corresponds to the southern margin of the Abukuma Mountains, which are composed of Cretaceous granite and schist (Abukuma granites and metamorphic complex, Geological Survey of Japan, AIST, 2012, see Data and Resources section; Fig. 1). The swarm zone bounds low hills underlain by Tertiary sedimentary rocks to the west. No major active fault has been mapped in the area, but several isolated fault strands shorter than 20 km were identified. These fault strands were interpreted

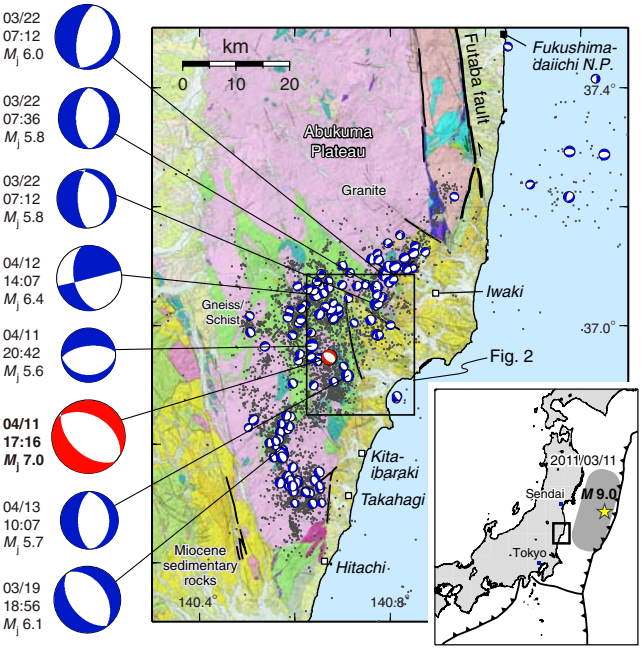

Figure 1. Focal mechanisms of large shallow earthquakes in the southeast Fukushima and northern Ibaraki areas after the Tohoku-oki (M_w 9) mainshock (F-net catalog from NIED, depth ≤ 20 km, M_j ≥4.0, 11 March 2011 to 10 August 2011), including the M_w 6.6 11 April 2011 Iwaki earthquake. Earthquakes that occurred after the Tohoku-oki mainshock (depth ≤20 km, M_j ≥2.0, 11 March 2011 to 10 August 2011), small dots. The location of Figure 2, dotted rectangular box. The geological map behind the earthquake plots is from the Seamless Digital Geological Map of Japan (Geological Survey of Japan, AIST, 2012; see Data and Resources section) and shows that swarm activity has been occurring in and around the boundary between Mesozoic granite/metamorphic rocks and Neogene sedimentary rocks. Mapped active faults (Research Group for Active Faults in Japan, 1991), thick black lines. The inset map shows the relationship between the M_w 9 source fault (gray) and the Fukushima region (box). The color version of this figure is available only in the electronic edition.

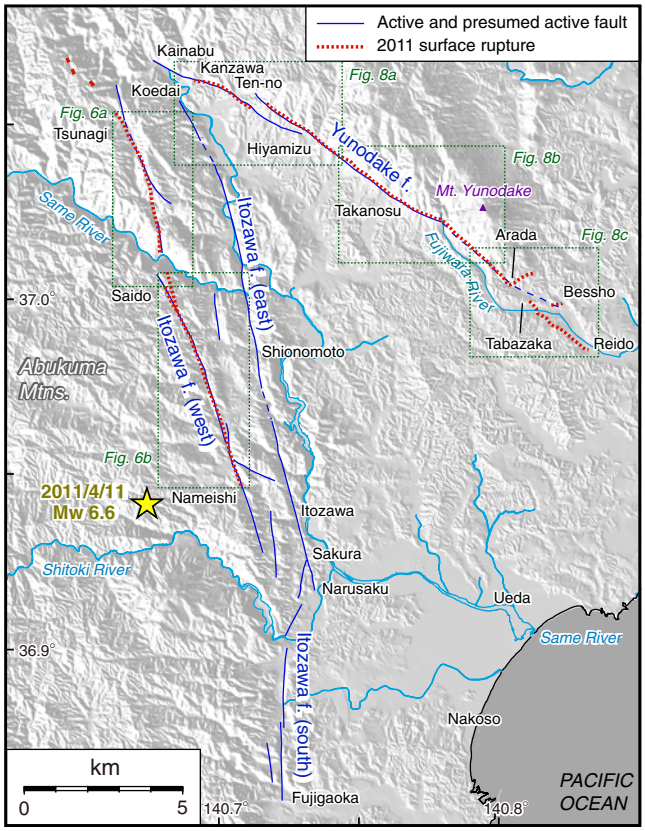

Figure 2. Spatial relationship between the surface rupture of the 2011 Iwaki earthquake and the active and presumed active faults identified in this study from aerial photograph interpretation. The shaded relief map was constructed using a 10-m-mesh digital elevation model by Geospatial Information Authority of Japan (GSI). The locations of Figures 6 and 9 detailed rupture maps are shown. The color version of this figure is available only in the electronic edition.

to be potentially active without discernible slip sense (Research Group on Active Faults of Japan, 1991; Nakata and Imaizumi, 2002). On 11 April 2011, a month after the Tohoku-oki mainshock, the largest normal-faulting event of M_w 6.6 (Japan Meteorological Agency magnitude [M_j] 7.0), officially named the Fukushima-ken-hamadori-no earthquake by the Japan Meteorological Agency (JMA; hereafter, Iwaki earthquake), occurred at the center of the swarm zone, where it triggered numerous rock falls and landslides, caused structural damage, and killed four people. The Iwaki earthquake involved multiple traces of surface rupture on mountain slopes and lowlands northeast of the epicenter. Two ~15-km-long subparallel ruptures appeared along the previously mapped Itozawa and Yunodake faults (Fig. 2).

In this paper, we describe the surface ruptures (location and slip distribution) of the Itozawa and Yunodake faults associated with the 11 April 2011 M_w 6.6 earthquake. We also note that these surface breaks were associated with existing active geomorphic features along reactivated geologic boundaries originally developed as a half-graben in the Neogene Period. We then report evidence for a penultimate surface-deforming earthquake sometime between 12,620 and 17,410 yr B.P. on the Itozawa fault, suggesting a long recurrence interval for such a forearc inland normal fault, and find no evidence for the Jogan A.D. 869 earthquake that is believed to be the penultimate giant megathrust earthquake along the Japan trench.

Tectonic Setting of the Epicentral Area of the Iwaki Earthquake

Tohoku, the northern part of Honshu island, is located west of the Japan Trench where the Pacific plate has been subducting westward beneath the Eurasian plate at a rate of ~8.0 to 8.5 cm/yr (DeMets *et al.*, 2010). Onshore and offshore regions of Tohoku had been compressed in an EW direction, possibly during the past 3 Ma (Sato, 1994), due to a strong frictional stress exerted on the interface between the overriding and subducting plates (Fig. 1). Despite ~200-yr complete historical records, relatively short compared to those of other regions of Japan, numerous M ≥7 megathrust

events along the plate interface, including the M_j 8.3 1896 Meiji Sanriku earthquake, have been recorded. Offshore from Sendai, Miyagi Prefecture, M_j 7 to M_j 8 shocks occurred in 1793, 1835, 1861, 1897, 1936, and 1978 with an average recurrence interval of 37 years. The Headquarters for Earthquake Research Promotion (2011) computed a 99% probability of an $\sim M$ 7.4 earthquake (possibly M 8.2 if it involves adjacent segments) for the next 30 years. The 11 March 2011 M_w 9.0 Tohoku-oki earthquake indeed initiated from the offshore Miyagi region but propagated bilaterally down to the offshore Ibaraki region, rupturing an ~500-km-long and 200-km-wide plate interface (Ide *et al.*, 2011; Simons *et al.*, 2011).

Significant EW contraction across the Tohoku region has been detected at different time scales, from decadal time scales based on continuous Global Positioning System (GPS) observations (Suwa *et al.*, 2006) and triangulation networks (Hashimoto, 1990) to geological time scales based on slip rates of active faults (Wesnousky *et al.*, 1982; Nohara *et al.*, 2000). The geodetic rate of contraction, however, is much greater, by one to two orders of magnitude, than the geologic rate. North- and northeast-trending active thrust faults, bounding basins, and ranges of inland Tohoku are interpreted to have accommodated such long-term crustal shortening during the late Quaternary. Recent destructive reverse-faulting earthquakes, such as the 2004 M_w 6.6 Chuetsu, the March 2007 M_w 6.7 Noto-hanto, the July 2007 M_w 6.6 Chuetsu-oki, and the 2008 M_w 6.9 Iwate-Miyagi-nairiku earthquakes, have proven secular EW compressional stress in inland Tohoku.

It is important to note that most of these destructive events were caused by steeply dipping reverse faults. The faults are reactivated normal faults that developed originally as rift-bounding faults associated with the opening of the Japan Sea during the Tertiary Period. Such "inversion tectonics" of inland Tohoku have been confirmed by recent large inland shocks (e.g., Kato *et al.*, 2005), seismic reflection surveys (e.g., Sato *et al.*, 2007), and offshore explorations along the eastern margin of the Japan Sea (e.g., Okamura *et al.*, 2005).

The Hamadori region is also characterized by a suite of half-graben structures developed during the Tertiary Period (Mitsui, 1971). The region was also famous for the Joban coal mine that had been booming until the 1970s. Active and presumably active faults are reactivated normal faults bounding individual half-graben structures infilled by >1 km of sediments (Fig. 3). These sedimentary rocks consist mainly of sandstone and siltstone units interbedded with coal seams, conglomerates, and tuffs. In the Quaternary Period, these units, in turn, have been subjected to EW compression and folded about axes plunging north–south (NS) to ~north-northwest (NNW)–(south-southeast) SSE (Mitsui, 1971). The basement rocks underlying the Neogene sedimentary rocks in the study area are Mesozoic metamorphic rocks that have also been strongly deformed. The Yunodake fault marks the southwest escarpment of the Abukuma highland, which

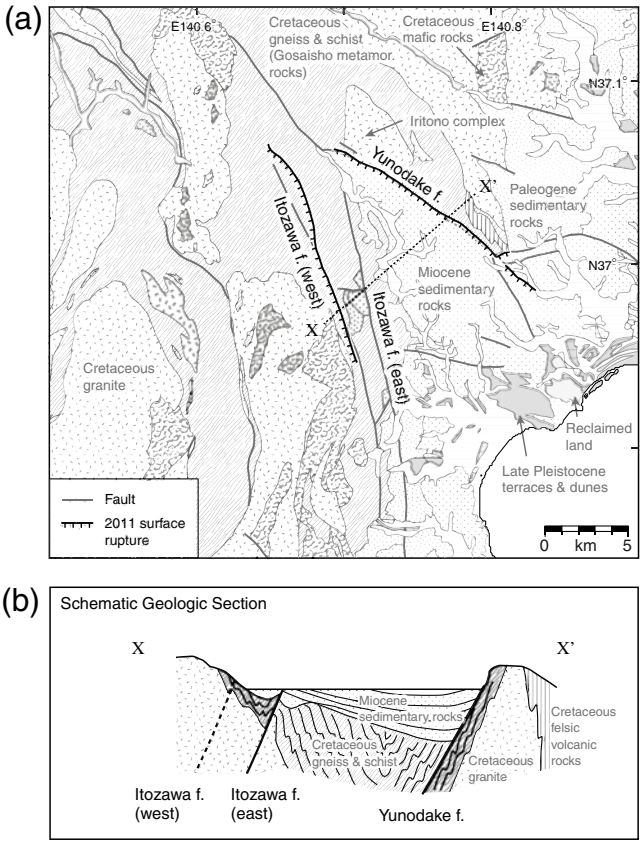

Figure 3. (a) Detailed geologic map in and around the surface rupture of the Iwaki earthquake (The Seamless Digital Geological Map of Japan, AIST, 2012). The 2011 rupture emerged mostly along previously mapped geologic faults. (b) Schematic geologic cross section along X-X′ from Mitsui (1971).

is composed of a massive Cretaceous granitic body and metamorphic rocks juxtaposed against the Neogene sedimentary units. Several small channels and gullies across the 2011 surface rupture expose the fault contact between schist and younger sandstone intercalating several millimeter-to-centimeter-thick fault gouges that prove that the faulting movements have repeated (Lin *et al.*, 2012). The geologically defined Itozawa fault (Mitsui, 1971) corresponds to the eastern strand of the two parallel geomorphically defined strands of the Itozawa fault (Research Group on Active Faults of Japan, 1991; Nakata and Imaizumi, 2002; Itozawa fault [east] in Fig. 2), which partially juxtaposes Neogene sedimentary units against the metamorphic rocks (Fig. 3). The western strand of the Itozawa fault (Itozawa fault [west] in Fig. 2) was mapped by Kano *et al.* (1973) as a major geological fault. Hereafter, for simplicity, we refer to the western strand of the Itozawa fault as simply the Itozawa fault. The triangular region bounded by the eastern Itozawa fault and the Yunodake fault is a hilly landscape composed of Tertiary sedimentary units, which show high contrast to the steep, rugged mountainous area composed of Mesozoic metamorphic rocks and granites to the north and west.

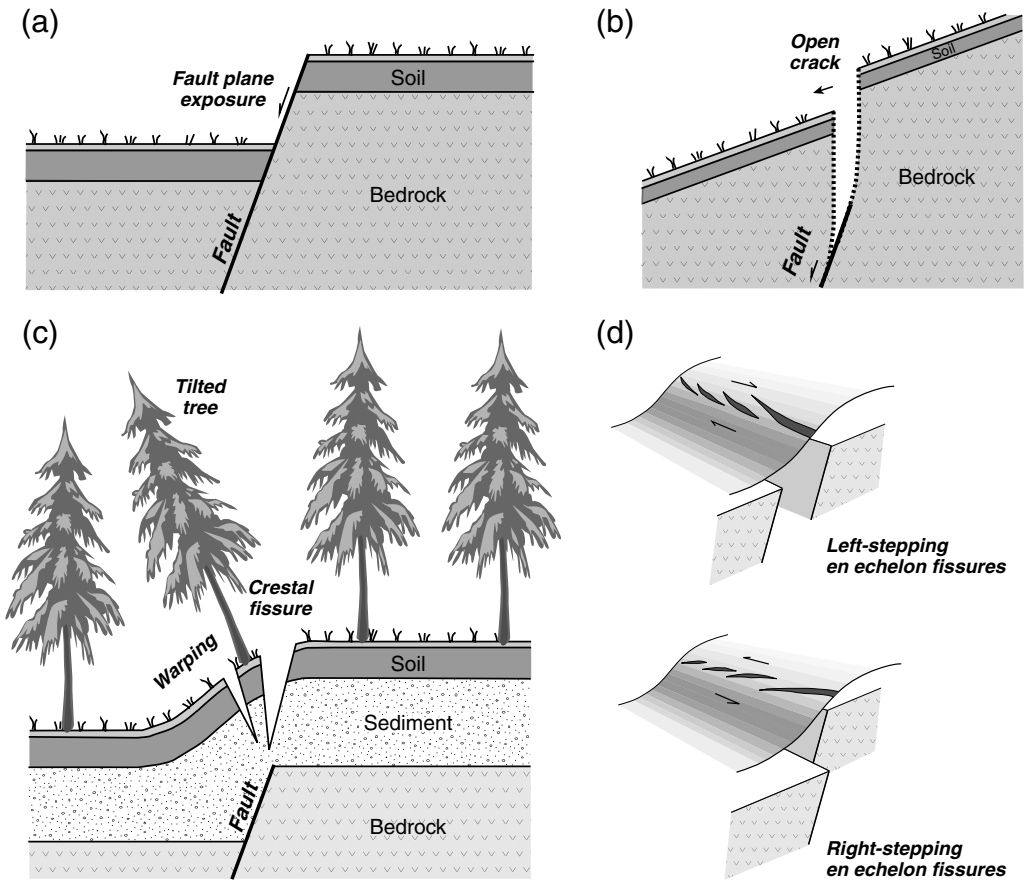

Figure 4. Schematic illustration of morphological types of the 2011 surface rupture. (a) Simple bedrock faulting exposing a free face of the fault plane on a flat ground surface or along a range-facing scarp. (b) Bedrock faulting on a steep slope involving fissures (open cracks). (c) Warping or gently dipping scarp involving crestal fissures occurring in sediment. (d) Alignments of crestal fissures associated with right-lateral (upper) and left-lateral (bottom) slip.

Observations of the 2011 Iwaki Surface Rupture

Timing and Methods of Observations

Several website reports were made of the surface rupture of the Iwaki earthquake immediately after the earthquake (Anan *et al.*, 2011; Ishiyama *et al.*, 2011; Kurosawa *et al.*, 2011). Ideally, mapping of surface ruptures and determining offset measurements should be done while the surface breaks are fresh and intact. Except for several key cultural features in populated areas that mostly were fixed immediately, however, ruptures in mountains and bushy hills are well preserved in our study area. We began by observing several easily accessible offset cultural features on 16–17 April 2011 and then mapped and measured the surface rupture from 27 April to 1 May, 20–23 June, and 1–4 November, a combined period of about two weeks.

For mapping, we used 1:25,000 scale topographic maps published by the Geospatial Information Authority of Japan (GSI). We used handheld GPS receivers (Garmin GPS map 60CSx) to locate observation points. To measure coseismic slip, two methods with different levels of measurement accuracy were used depending on the local conditions and our limited survey time: (1) we measured vertical and horizontal offsets of the ground surface and some piercing objects using a conventional tape or folding ruler and hand level mostly on mountain slopes; (2) we used an auto-level to take cross-sectional profiles of offset cultural features such as paved roads, dirt roads, and rice paddy dikes. When we encountered bedrock exposures along the rupture zones, we recorded fault strike and dip. We also measured the direction of striations (rake) where such features were clearly observable.

During the latter stage of our field survey, we used Interferometric synthetic aperture radar (InSAR) images (GSI, 2011; Fukushima *et al.*, 2012) to facilitate identification of the rupture. We also used these to find minor displacements associated with the other interferogram fringe offsets. For instance, short breaks and cracks were confirmed at spot locations along the eastern strand of the Itozawa fault.

General Features of the Surface Rupture

A variety of morphological styles of surface rupturing were observed (Fig. 4). The most frequently occurring rupture type was a gently to steeply warped or monoclinal scarp

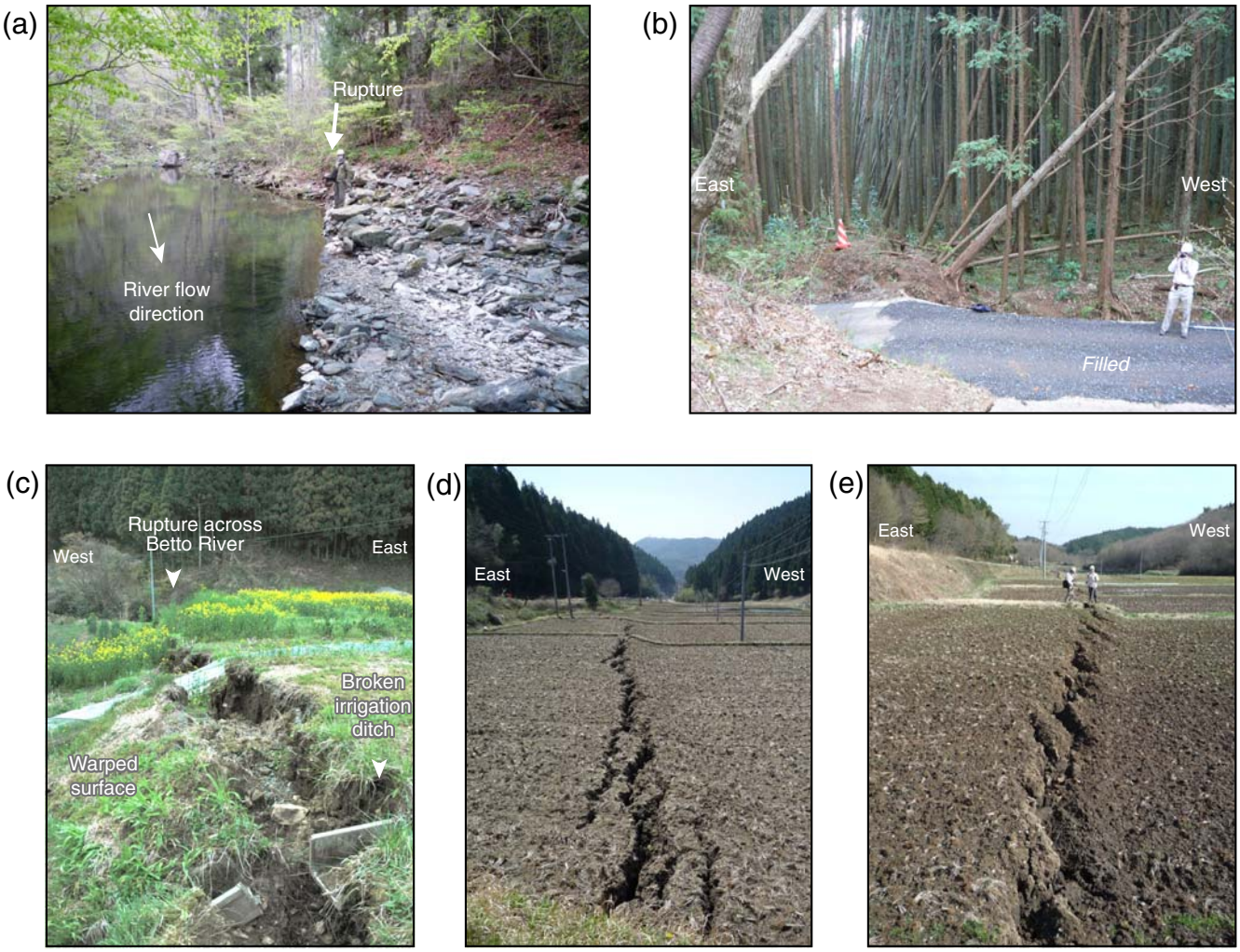

Figure 5. Photos of the 2011 surface rupture. (a) A fresh fault scarp obliquely cut the Kiyodo River, exposing dried basal gravel on the downstream side. (b) A swath of fallen and tilted cedar trees on the fresh scarp associated with the 2011 rupture at a location ~1 km north of our trench site. The downthrown side was already filled and flattened when the photo was taken (see the graveled path beneath the person). (c) 1-m throw and crestal fissures broke the irrigation canal at the Kakehashi trench site (photo taken on 27 April 2011). (d) Left-stepping en echelon cracks, suggesting a small right-lateral component of slip, on the crest of the warped scarp formed by the 2011 earthquake at Nakano, southern part of the Itozawa fault. Footpaths across the rice paddies were confirmed to have dextral offsets. (e) Right-stepping en echelon fissures along the fresh scarp at Shionohira. Footpaths across the rice paddies are displaced sinistrally. The locations of these photos are shown in Figure 6. The color version of this figure is available only in the electronic edition.

including tension fissures on the crest (Figs. 4c and 5c). This type of rupture characteristically appeared where there were thick unconsolidated sediments and/or soil units, mostly in alluvium. When there was a component of lateral slip, left-stepping (right-lateral slip) and right-stepping (left-lateral slip) en echelon fissures were observed (Figs. 4d and 5d–e). We confirmed that these senses of en echelon alignment were consistent with lateral offsets measured from nearby cultural features. When a significant amount of vertical slip (> 1 m) occurred in bedrock, a combination of fault free face (Fig. 4a) and colluvial wedge (debris slope) was frequently observed. Tilted trees were commonly seen along rupture zones. The trees often emphasized the ground deformation (Figs. 4c and 5b) and became a clue to following the rupture zone in forested mountains. Clear and fresh scarps were observed at bedrock sites (Fig. 4a) and often exposed remarkable or ambiguous striations. The free faces occasionally exposed a fault gouge zone, mostly thinner than 1 cm. Along the steep bedrock slope of Mt. Yunodake and consistent with the dip direction of the Yunodake fault, we regularly observed open cracks as wide as 1 m, which are the result of gravitational collapse/movements and are equivalent to landslide scars (Fig. 4b).

We commonly observed larger vertical displacements at the bottom of gullies than at ridge crests in mountainous locations (i.e., the detailed slip distribution west of Mt. Gosaisho in Fig. 6b). This might be due to near-surface tapering of coseismic slip or to differences in overburden stress.

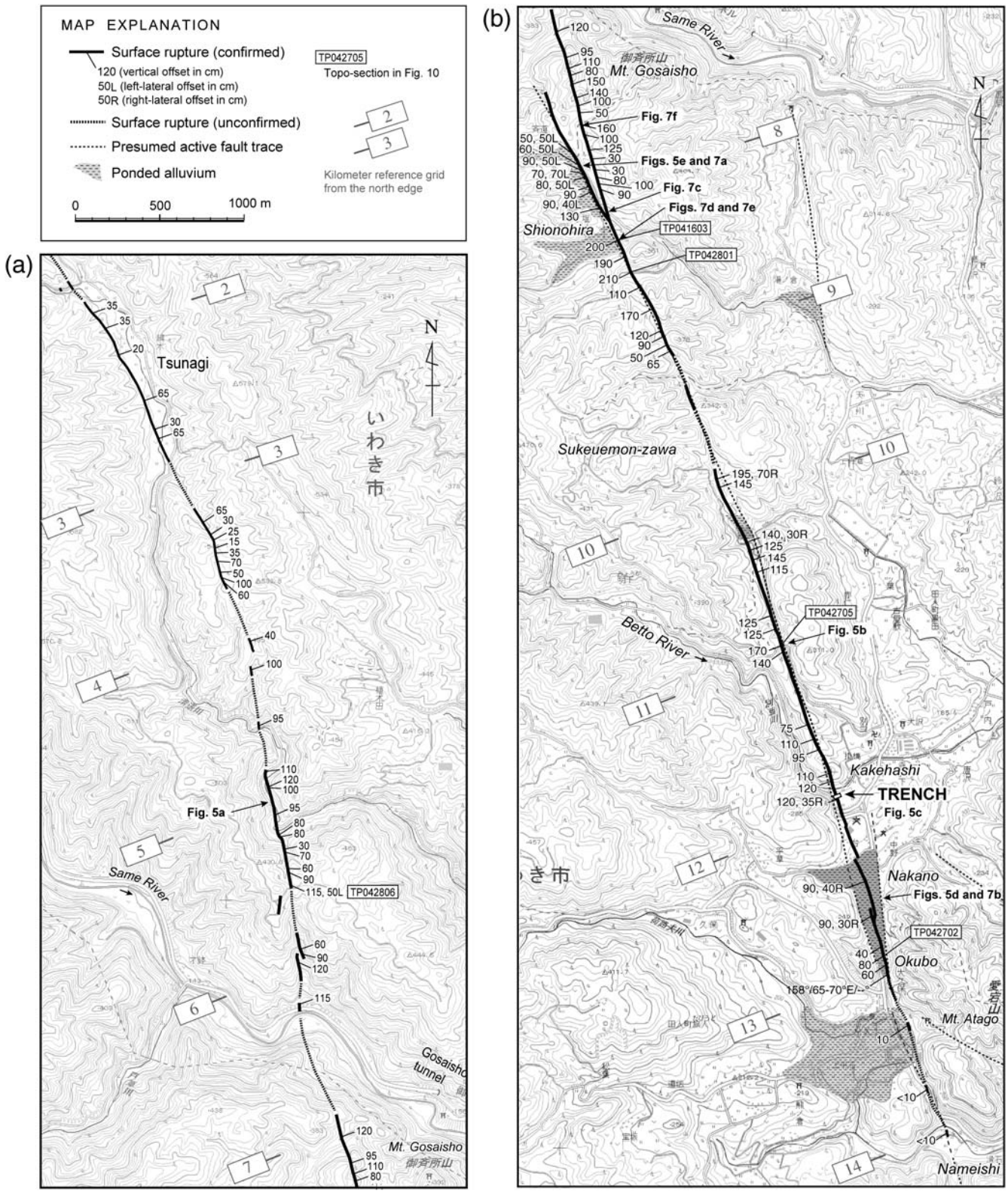

Figure 6. Strip maps of the 2011 rupture along the Itozawa fault. Fault sections with tectonic geomorphic features delineated by aerial photograph interpretation are also shown. The basemap is the 1/25,000 topographic maps *Kamihiraishi* and *Katono* published by Geospatial Information Authority of Japan (GSI).

Figure 7. Photos of the 2011 surface rupture along the Itozawa fault. (a) Oblique aerial view to the south of the central part of the 2011 rupture zone, cutting across a rice paddy field at Shionohira. Fault saddles along which the rupture appeared, open triangles. Note that water ponded along the fault scarp on the downthrown side (Fig. 7c–d). Photo taken by Go Sato, Teikyo Heisei University. (b) Oblique aerial view to the south at Nakano. 100-m-order surface traces are stepped as well as the meter-order steps (Fig. 5e). Notice the contrast of moisture content over the rupture. The downthrown side may have been soaked due to the sudden interruption of groundwater flow after the earthquake. Photo taken by Go Sato, Teikyo Heisei University. (c) Fault scarp of the western strand of the Itozawa fault that is <1 m high at Shionohira. The downslope side of the rice paddy field was uplifted and the downthrown side was filled by water. (d) Approximately 2-m-high fault scarp along the western strand of the Itozawa fault exposing the bedrock fault plane at Shionohira. (e) Close-up view of a part of the exposed fault plane shown in (d). The oblique slip striations on the fault plane are consistent with the measured oblique slip. (f) Near-vertical free face of the 2011 fault scarp exposed toward the mountain slope side. A small pond was formed by the damming movement of the Itozawa fault. The locations of these photos are shown in Figure 6. The color version of this figure is available only in the electronic edition.

Surface Rupture along the Itozawa Fault

An ~14-km-long NNW-trending surface rupture appeared along part of the western strand of the Itozawa fault. The sense of vertical slip is up to the east, which raises the downslope side of the mountain foothills and forms range-facing normal fault scarps. Thus, most of the rivers and small channels across the rupture zone were dammed (Fig. 5a), and some flooded after the earthquake. This suggests that the fault movement during the Iwaki earthquake was in the opposite sense to the large-scale topography. The fault crosses undulating topography, but the trace of the 2011 rupture zone is fairly straight and not influenced by sinuous topographic contours. This implies that the dip angle of the Itozawa fault is steep, roughly consistent with the observed dip of ~70° or greater on bedrock free faces of the 2011 rupture (e.g., Fig. 7d–f). Although fault branching occurred at Shionohira, the center of the entire rupture zone, the fault zone otherwise has clear continuity. The maximum vertical slip of 2.1 m was measured at Shionohira (8.5 km mark; Fig. 6b). The shape of the slip distribution is an asymmetric chevron that linearly

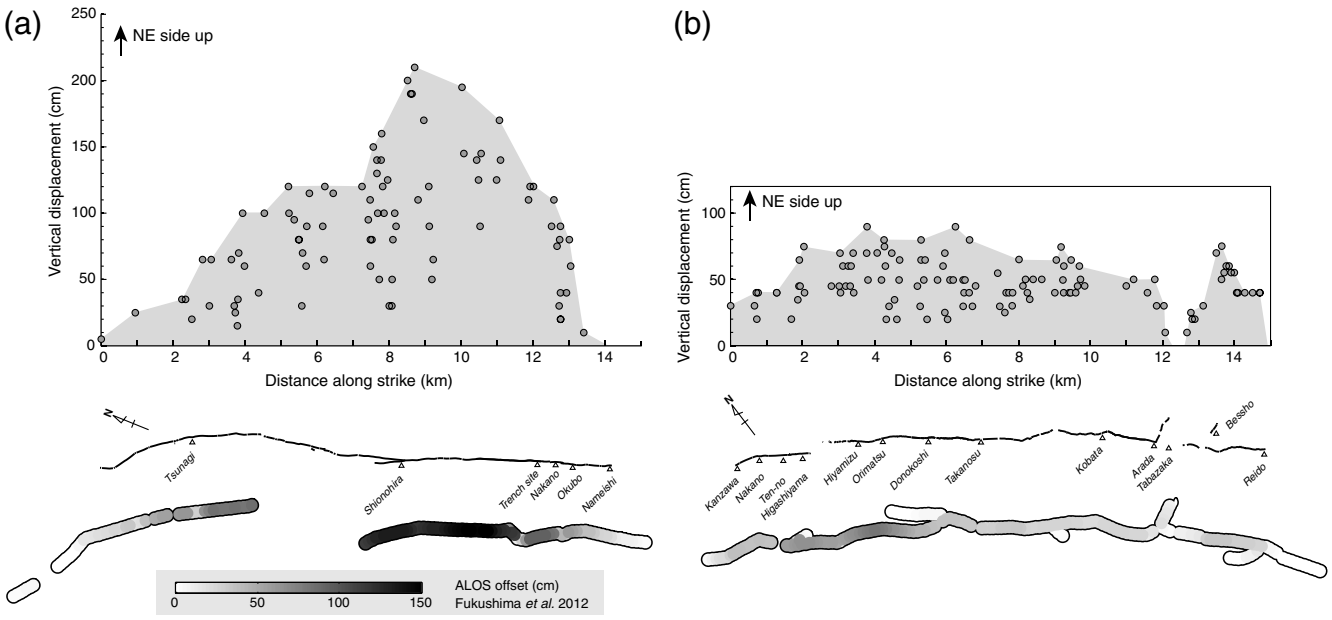

Figure 8. Distribution of vertical slip (upper panels) and plan view (middle panels) of the surface rupture of the (a) Itozawa and (b) Yunodake faults during the 2011 earthquake. Possible maximum field displacements along the rupture zones are preferentially selected and shown in gray. The lower panels are measured LOS (line-of-sight) offsets obtained from discrete fringes of InSAR analyses with data from the Advanced Land Observation Satellite (ALOS; Fukushima *et al.*, 2012). The distribution and tendency of the measured field offsets are similar to those by LOS displacements, which are estimated to be ~60% of the net slip along the rupture zones (Fukushima *et al.*, 2012). The edges of the rupture zones detected by the interferograms, however, extend 1 to 4 km farther from the edges of our discernible rupture traces.

tapers toward the edges (Fig. 8a). Because the maximum displacement is located ~1.5 km south of the center (at 8.5 km), the degree of tapering toward the southern edge is steeper than toward the northern edge (Fig. 8a). A left-lateral component of up to 70 cm is observed on the rupture zone north of Shionohira (8.1 km), whereas a right-lateral component up to 70 cm is measured along the rupture zone south of Sukeuemonzawa (9.9 km; Fig. 6b). The southern part of the Itozawa rupture zone mostly has right-lateral slip of one-third to one-half the magnitude of the vertical component. A dislocation model in an elastic half-space, which pulls the Earth's surface toward the center of the hanging wall, clearly explains such a symmetric pattern of lateral displacement.

Surface Rupture along the Yunodake Fault

A surface rupture 15 km long appeared on bedrock along the Yunodake fault during the Iwaki earthquake. The overall vertical slip sense is northeast side up, which, unlike that of the Itozawa fault rupture, is consistent with the large-scale topography. The general trend of the rupture zone is N50°W. Although the rupture is mostly on a single strand, detailed traces of the rupture zone are complex and include a distinct 0.4-km step, a couple of 90° bends, and a 0.5-km gap. In the northern part of the rupture zone (Kanzawa to Higashiyama; 0 to 2.1 km marks), a 2-km-long continuous, linear surface break with vertical displacements up to 80 cm was observed (Fig. 9a). The rupture terminated at Higashiyama (2.1 km) and jumped to Hiyamizu (2.6 km), displaying a 0.4-km step and 0.5-km gap. This rupture transfer indeed followed the inferred stepover of the fault sections (dashed line in Fig. 9a) characterized by a series of saddles with systematic left-lateral deflection of channels associated with long-term fault motions. The ~9-km rupture zone from Hiyamizu to Arata (2.6 to 11.8 km marks) is characterized by a linear but moderately sinuous trace along a geomorphic boundary between the mountain slope and gentle foothills, which is also a boundary between granite/metamorphic rocks and Neogene sedimentary rocks (Fig. 3). Along this section, the amount of vertical displacement ranges from 20 to 90 cm with a subtle left-lateral component. At Arata (11.8 km), about 0.5 km west of the Iwaki-Yumoto interchange of the Joban Expressway, the rupture trace bends 90° toward the northeast (Fig. 9c), sustaining the north-side-up movement. The east-northeast (ENE)-trending rupture is traceable for at least 0.7 km with accompanying right-lateral slip of 10–20 cm, which might be a conjugate relation with the small left-lateral slip along the northwest (NW)-trending main section. We could not find any breaks in the area between Arata and the Iwaki-Yumoto interchange of the Joban Expressway (11.8 to 12.5 km marks), which indicates a 0.7-km gap in the rupture. Southeast of the gap, a 2.5-km-long southernmost section of the rupture (12.5 to 15 km) emerged across several river terraces and the alluvial plain along the Fujiwara River. The fault section here is more sinuous than the rest of the Yunodake rupture zone but retains NE-up vertical slip. At Bessho, we observed an ENE-trending,

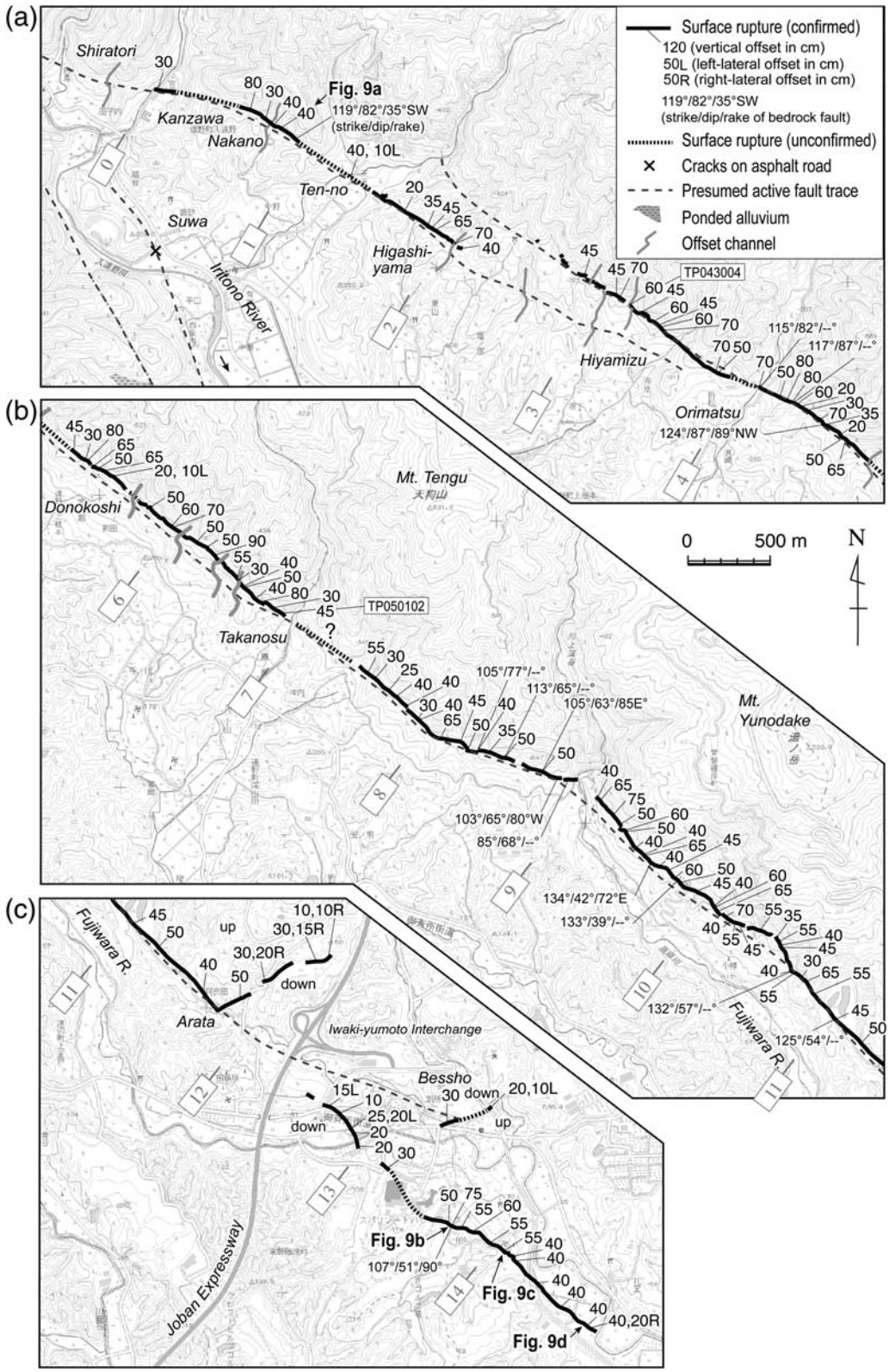

Figure 9. Strip maps of the 2011 rupture along the Yunodake fault. See Figure 2 for the locations in the entire 2011 rupture zone. Fault sections with tectonic geomorphic features delineated by aerial photograph interpretation are also shown. The basemap is the 1/25,000 topographic maps *Katono*, *Joban-Yumoto*, and *Joban-Izumi* published by Geospatial Information Authority of Japan (GSI).

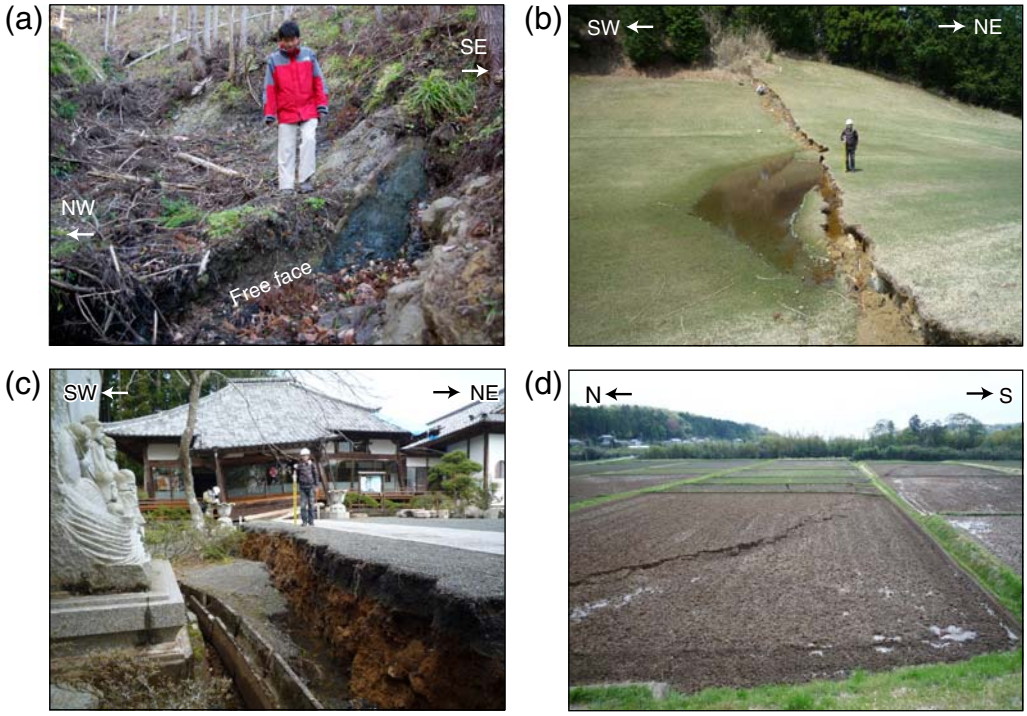

Figure 10. Photos of the 2011 surface rupture along the Yunodake fault. (a) Fresh free face of the bedrock fault across a channel at Nakano, on the northern section of the Yunodake fault. Dip of the fault is 70°. Barely-visible striations of ~90° suggest no lateral slip component. (b) Fresh scarp cutting across a golf course. (c) An entrance path and a tilted temple due to a 60-cm vertical displacement. (d) Surface rupture involving crestal open cracks at the southern end of the Yunodake fault. The locations of these photos are shown in Figure 9. The color version of this figure is available only in the electronic edition.

~0.4-km-long minor rupture zone with south-side-up displacement of 30 cm, which may be a smaller version of the conjugate trace observed at Arata. As the rupture along this section cuts across residential areas, several houses and buildings were broken and tilted due to the coseismic slip (Fig. 10c).

The maximum vertical slip of 0.9 m was measured at Takanosu (6.3 km). The shape of the slip distribution is plateaulike, however, unlike the chevron shape of the Itozawa rupture zone (Fig. 9). The southernmost 2.5-km-long rupture does show a small chevron with 75 cm of maximum vertical displacement at the center. We rarely observed piercing points at which we could reliably measure lateral slip and most of these showed ~10 cm of left-lateral offset along the NW–SE main rupture section. As noted above, two minor ENE-striking sections are characterized by right-lateral displacement.

Surface breaks along the Yunodake fault occurred mostly on bedrock, so the free face of bedrock fault exposures was observed at many locations (see the strike, dip, and rake information on the fault exposures in Fig. 9). Dip angles measured in the northern section are extremely high, ranging from 82° to 87°, which is consistent with the linear rupture trace, whereas those along the central section range from 39° to 77°. The moderately dipping fault was often associated with open fissures at the surface (Fig. 4b).

Tectonic Geomorphic Features of the Yunodake and Itozawa Faults

In addition to our field observations of the surface rupture, we also mapped the surface trace of the Yunodake and Itozawa faults based on aerial photograph interpretations. We used black-and-white aerial photographs with scales of 1:20,000 and 1:40,000 taken by Geospatial Information Authority of Japan in the 1960s and 1970s. Figure 2 shows the active and presumed active fault sections with geomorphic features indicative of late Quaternary faulting. The Yunodake fault consists of two main sections. The northwestern section is ~5 km long and extends from Kainabu to Hiyamizu. The section is characterized by a series of saddles on ridges and left-laterally offset streams with deflections as large as 50 m. The coseismic rupture appeared along part of the fault section from Kanzawa to Higashiyama (Fig. 9a). The southeastern section of the Yunodake fault is ~11 km long and located at the sharp topographic boundary between mountain slope and hills. The southeastern section runs parallel to and overlaps the northwestern section for a distance of 2 km with an ~300-m stepover between the sections (Fig. 9a). Surface rupturing did not occur at the eastern end of the northwestern section or the western end of the southeastern section, leaving a 500-m-long gap in surface rupture east of Higashiyama. The southeastern section is characterized

by well-defined tectonic geomorphic features, such as shutter ridges, stream offsets, and beheaded rivers. Systematic left-lateral stream offsets are observed west of Takanosu, and the maximum offset is ~100 m. The Yunodake fault runs across hilly terrain and young geomorphic surfaces such as alluvial plains and fans, which are critical for identifying recent movement of the fault, but these are sparsely distributed. Nonetheless, the systematic left-lateral offset of streams implies that the Yunodake fault moved repeatedly during the late Quaternary. We cannot identify any tectonic geomorphic features along the surface rupture east of the Joban Expressway.

The Itozawa fault consists of three main sections (Fig. 2). The total length of the fault is ~23 km. The eastern section, extending from Koedai southward to Narusaku, is fairly straight and continuous. The southern section branches from the eastern section at Sakura and extends southward to Fujigaoka. The southern section is composed of short en echelon faults. The western section is straight and continuous from Saido to Sakura but is discontinuous north of the Same River. All the sections of the Itozawa fault are characterized by west (upslope)-facing scarps. Because of the uplift of the downstream sections of east-flowing rivers, many elongated, ponded alluvial plains exist along the fault. No tectonic scarp exists on these alluvial surfaces, however, suggesting that the fault has not moved in the past several thousand years. In contrast to the Yunodake fault, we could not identify systematic lateral offsets of streams. The 2011 surface rupture appeared along part of the western section of the Itozawa fault (Figs. 2, 6, and 11), leaving the 2-km-long southern end unruptured south of Nameishi.

Paleoseismic Trench across the Itozawa Fault

We exposed paleosesimic evidence across the 2011 rupture zone to reveal the earthquake recurrence interval of the Itozawa and Yunodake faults and potentially to help discern the timing of past Tohoku-oki type events. If the normal faults in the region move only under the extensional stress field induced by offshore *M* 9-class megathrust events, we may indirectly reveal the history of such megathrust earthquakes. The historical A.D. 869 Jogan and A.D. 1611 Keicho earthquakes are often referred to as candidates for previous *M* ~9 earthquakes along the Japan trench. Sawai *et al.* (2007) confirmed that flooding from tsunami events along the Sendai coast occurred during both the Jogan and Keicho earthquakes. The estimated sizes of the Jogan (*M* 8.3–8.6) and Keicho (*M* 8.1) earthquakes, however, are much smaller than that of the 2011 Tohoku-oki earthquake (Imamura and Anawat, 2012). There still might be a possibility, though, that the 869 Jogan earthquake was the penultimate event of the 2011-type megathrust earthquake, suggesting a "super cycle" (Sieh *et al.*, 2008) with a recurrence interval of about 1000 years. If so, the question of whether the Jogan earthquake was also accompanied by normal faulting earthquakes in the Hamadori region must be raised.

Trench Site and Exposed Stratigraphy

We chose a terrace on the southern bank of the Betto River at Kakehashi, Tabito Town, as our trench site (Fig. 12a). At the site, a fresh west-side-down throw (uphill-facing scarp) of 1.2 m with 0.3 m of right-lateral slip occurred during the Iwaki earthquake. The Betto River, about 50 m north of the trench site (Fig. 5c), was partially dammed by east-side-up coseismic movement. The land owner told us that the rice paddy of the trench site had been completely flat before the 2011 Iwaki earthquake. We thus expected to find dateable fine sediments from frequent river floods that had been well preserved as a result of such range-facing scarp-forming movements. We excavated a 15-m-long, 7-m-wide, and 3.5-m-deep trench across the 2011 fault scarp during September 2011. To maintain stability of the trench walls with the shallow groundwater level, we kept the slopes at about 70° (Fig. 13). We established an arbitrary grid system on the 70° slope. The locations of all features described in the trench are given according to our grid system. When describing the coordinates of a particular feature of the trench walls, we first present a horizontal meter mark coordinate for either the north or south wall (e.g., N8, S5), and then, if needed, follow it with a down-trench-slope coordinate in meters, as shown in Figure 13.

The trench walls exposed terrace gravels overlain by sand, silt, and humic soil layers deposited by the Betto River. Both walls also revealed 2011 surface breaks and ground-surface warping formed by a west-dipping, subvertical normal fault that offsets all of the stratigraphic units. We divided the sediments into 20 units based on composition, sedimentary facies, and structure. Our log of the southern and northern walls of the trench and brief descriptions of the stratigraphic units are given in Figure 13.

Fissures and fissure fills are observed at the apex of the 2011 scarp at N8 to N9.5 and at S8 to S9. Because our excavation was performed five months after the earthquake, the fissures had been filled by fine surface soil. One of the fissures (at S8 to S9) extends downward into units 20 and 30 and is filled with sand of unit 10. At S8 and N8, underlying subvertical faults exist about 50 cm west of the crestal fissures associated with the 2011 scarp. On the south wall, the fault splays upward, showing a positive flower structure like those typically observed across a strike-slip fault. The vertical separation of the top of unit 140 is about 40 cm, which is significantly smaller than the observed vertical separation of the ground surface. This suggests that the total fault slip was widely absorbed in the shallower units due to the stiffness contrast between the sediments, and only a fraction of the displacement was converted as the sharp offset of unit 140. The warping becomes much wider as it moves toward the ground surface. Vertical offsets are not evident in units 10 and 20. Instead, a 3-m-wide folding occurs in these

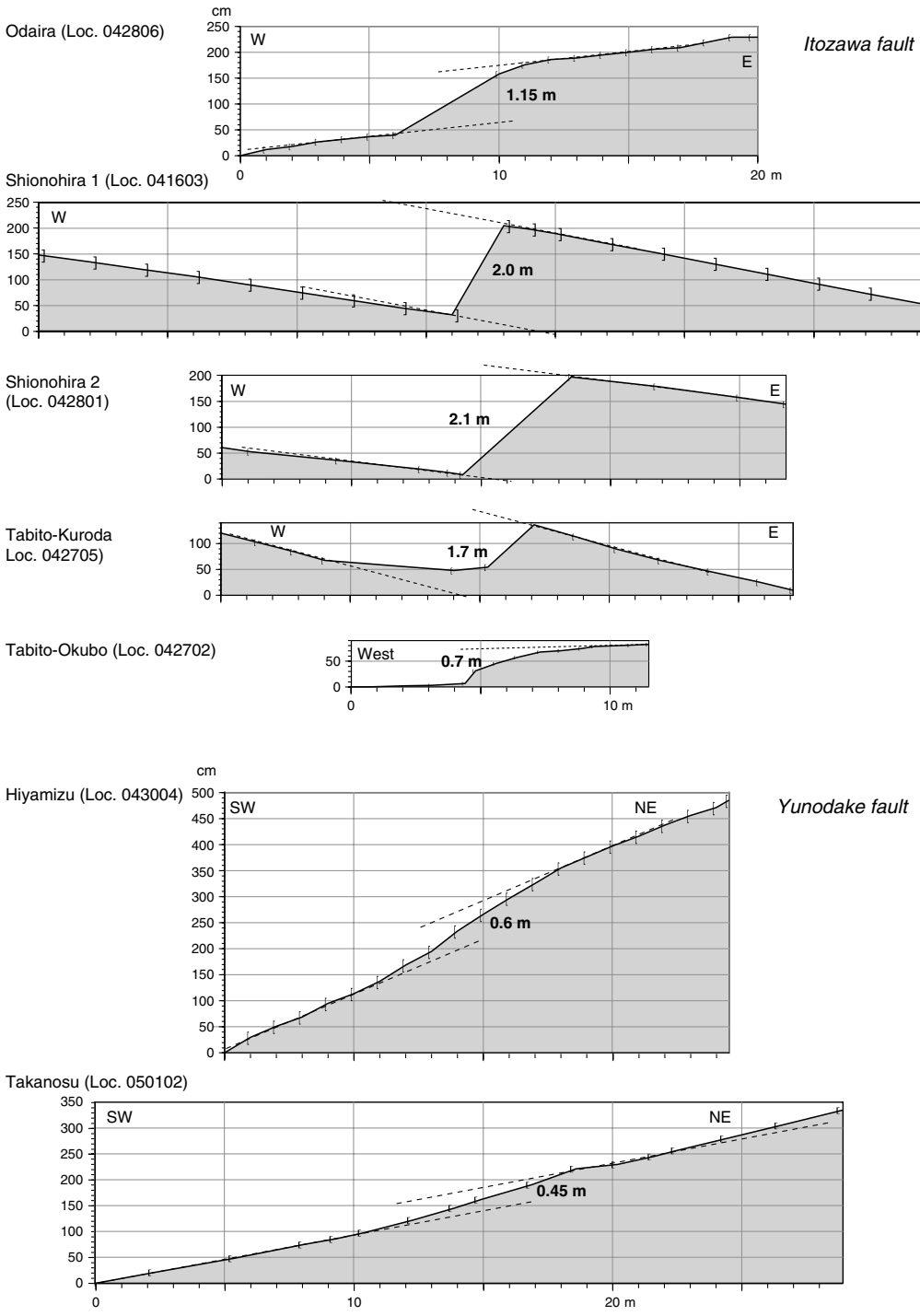

Figure 11. Measured cross sections of 2011 fresh fault scarps. Compass, tape, hand-level, and auto-level instruments were used to make the sections. The locations are shown in Figures 6 and 9. Note that uphill-facing scarps are evident across the Itozawa fault.

sedimentary units. On the north wall, the fault clearly extends into unit 10, although the offset is small.

Very recent channel cuts and fills associated with possible meandering of the Betto River were seen in the eastern part of the trench. Significant erosion associated with meandering is interpreted to have occurred after the deposition of unit 10. The depth of the channel erosion was about 2 m. A set of units, 2, 4, 6, and 8, that fills the channel shows a gradual fining-upward sequence. These observations suggest that the Betto River itself or a tributary temporarily flowed to the southeast.

At the western side of the trench, the very fine grained, organic-rich units 70, 80, and 90 are exposed only on the downthrown side of the fault. These units seem to have been

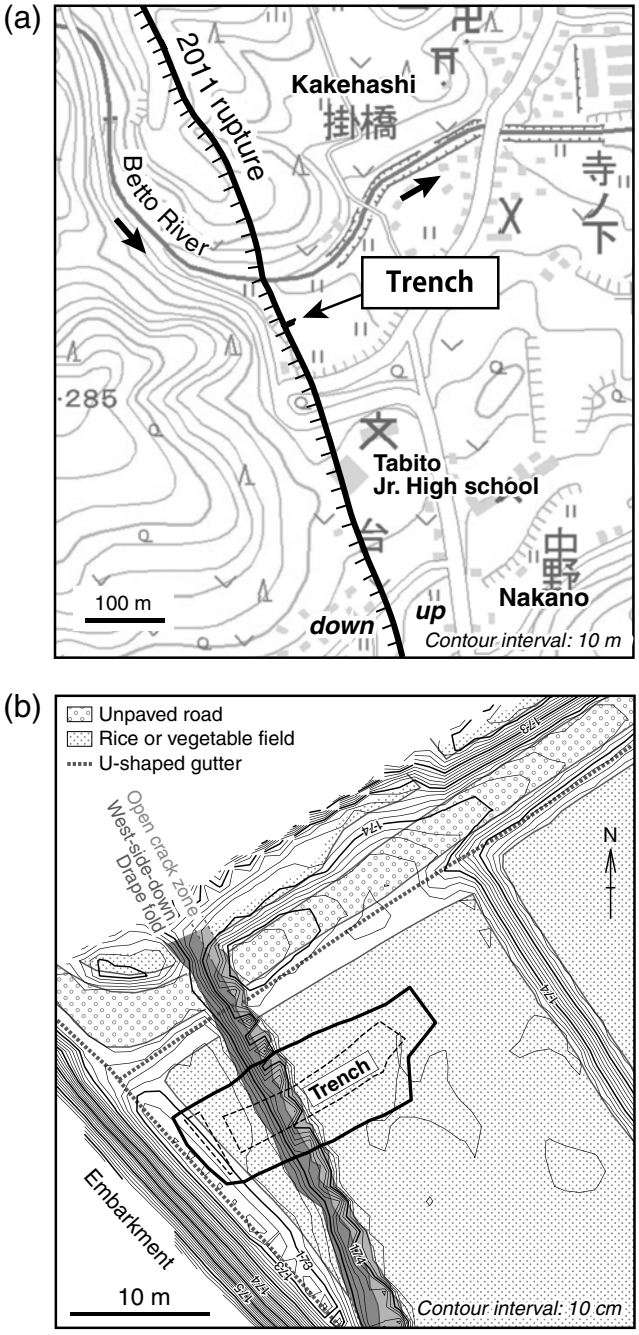

Figure 12. (a) Map of the location of our paleoseismic trench site across the 2011 rupture zone along the Itozawa fault. (b) Arrangement of the trench perpendicular to the warping scarp with crestal fissures.

deposited in a subtle basin related to the penultimate event. The gravelly sand units 40, 50, and 60 onlap the underlying units 70, 80, and 90 with sharp erosional contacts and are also exposed mostly on the downthrown side.

Thick gravel unit 140, which is primarily a fluvial deposit of the Betto River, underlies younger units composed of a variety of grain sizes ranging from silt to cobbles that formed as a result of periodic flooding, channel erosion, and channel filling. Units 110 and 120 are well-bedded sand layers that drape unit 140 with gradual contacts, which may suggest that these units were deposited during a short time period under the same fluvial conditions. The vertical displacements of the tops of unit 140 and unit 110 are about 1.5–1.7 m, which suggests that additional vertical movement might be recorded in lower stratigraphic units.

To constrain the depositional ages of these strata, we performed accelerator mass spectrometer radiocarbon (^{14}C) analyses on seven samples of detrital charcoal and wood fragments (Table 1). All samples were analyzed at the Institute of Accelerator Analysis, Ltd., Kanagawa, Japan. The ages range from ca. 7000 to 19,400 cal yr B.P. The age determinations are generally concordant with stratigraphic order (Fig. 13), suggesting that reworking of dated material can be ignored at the site. The age constraints suggest that unit 140 might be a product of the peak of the last glacial period and that sedimentation then occurred intermittently until the last sea level rise of the Holocene glacial retreat (~6000 yr B.P.).

Evidence for the Penultimate Event

Two pieces of evidence for the penultimate event were observed at the same stratigraphic horizon on the trench walls. One is the unconformity associated with faulting. The other is paleoliquefaction and fluidization, possibly due to strong shaking from a nearby source. Although units 10, 20, and 30 are warped like the ground surface with 1.1–1.2 m vertical offsets and flattening at S6, underlying units 110, 120, and 140 experienced larger vertical offsets, as much as 1.5–1.7 m, and the western edge of the deformation in these units is located farther to the west (S5). This suggests that the mode of deformation and the amount of vertical offset of the underlying group are distinguished from those of the overlying younger units. In addition, units 40 through 110 are preserved on only the hanging wall side, as mentioned above, filling a structural gap between units 110–140 and 10–30. Furthermore, a fissure fill that has characteristics similar to those of the 2011 surface cracks is discernable among units 90, 100, 110, and 120 at S4.5–5 and D3.6–4.2. On the north wall, a distinct flame and fluidized structure was observed in medium-to-coarse sand intercalated by black humic soil in the same stratigraphic units at N4, D3.5, which might also be evidence for strong ground motion (Fig. 14b). Based on these observations, we interpret the event horizon of the penultimate event to be the top of unit 70. We suppose that the penultimate event locally preserved the pre-event, near-surface peaty paleosol (units 70–90) and then promoted the additional sedimentation of units 40–60 into a pocket basin associated with the event. The measured offset of 30–40 cm associated with the penultimate event, however, is remarkably smaller than that of the 2011 event. The location of the paleofissures in units 90–120 and positioning of the basin (away from an apex of the paleoscarp) suggest that

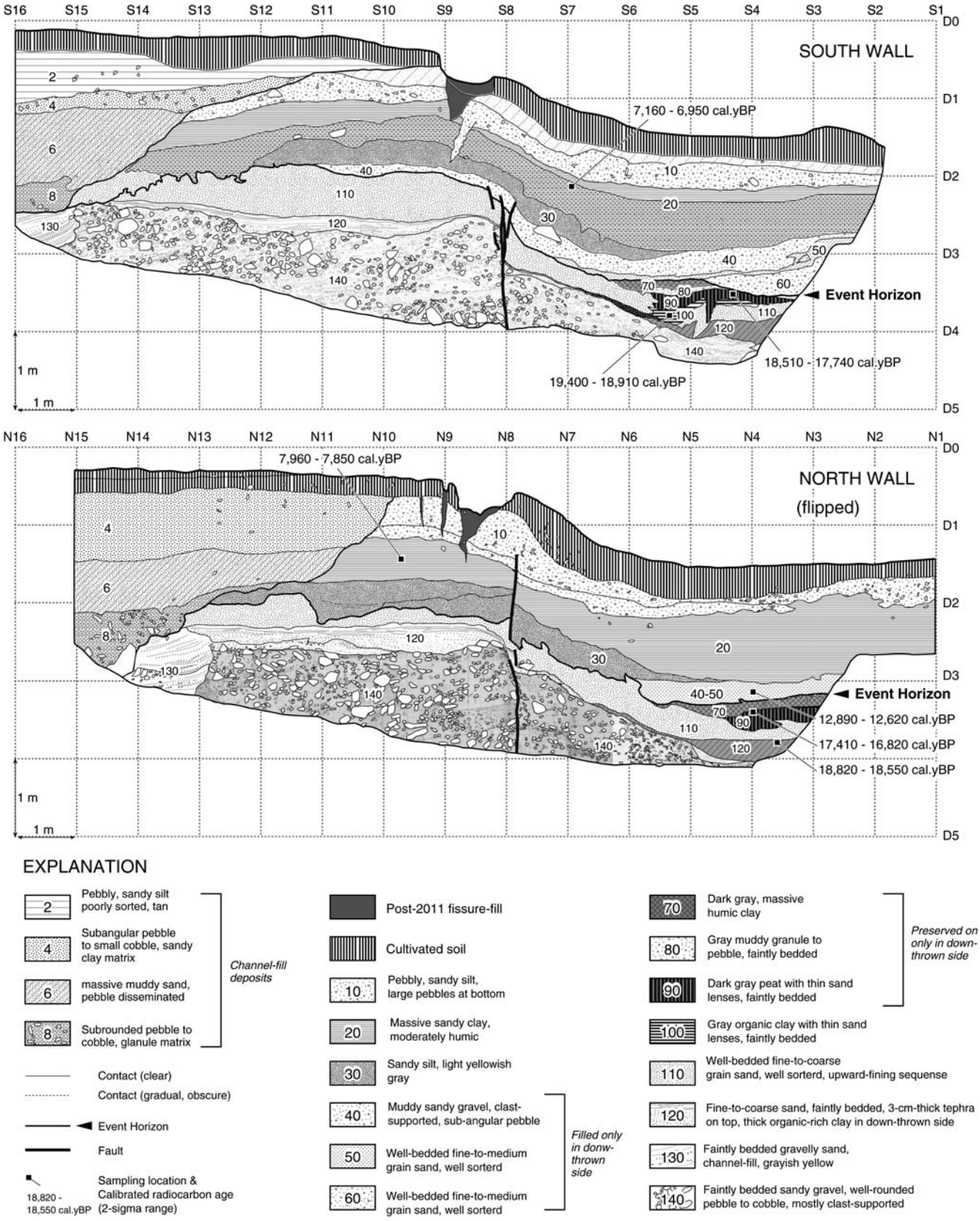

Figure 13. Cross sections of south and north walls of the trench at Kakehashi. The sections were taken along 70°-inclined walls so the vertical axis is faintly exaggerated in our grid system. Strata exposed in the trench show evidence for not only the 11 April 2011 Iwaki earthquake but also for the penultimate surface-deforming event on the *Event Horizon*. Radiocarbon dates were calibrated with the database of Reimer *et al.* (2009) on the OxCal v 4.1 software.

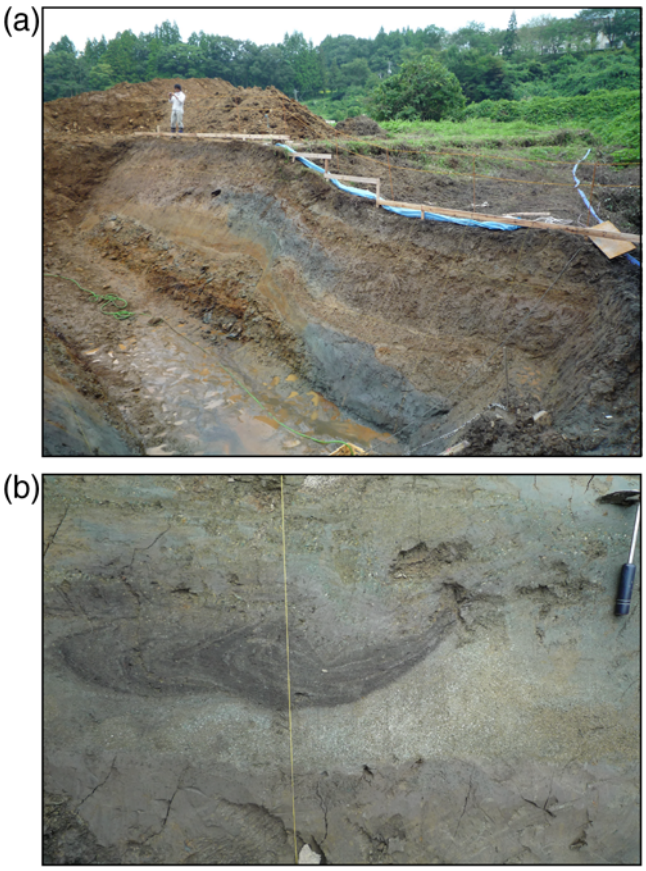

Figure 14. (a) Oblique view of the south wall of the trench across the Itozawa fault. (b) Fluidized sand and overlying peat units due to a large shaking event, which supports stratigraphic unconformity evidence for the penultimate surface-rupturing earthquake (*event horizon*). The color version of this figure is available only in the electronic edition.

the style of deformation associated with the penultimate event was quite different from that of the 2011 event.

Figure 13 and Table 1 show the 2-σ ranges of the ages of the samples calibrated with OxCal v 4.1. Units 90, 100, and 120 below the event horizon yielded an age of 19,400 to 16,820 cal yr B.P., whereas the samples above the event horizon dated from 12,890 to 6950 cal yr B.P. The youngest sample from the former group (KKH-N21) and oldest sample of the latter group (KKH-N20) bracket the timing of the penultimate event between 12,620 and 17,410 cal yr B.P. This time constraint is consistent with our geomorphological observation that no fresh scarp exists on the alluvial plains. It also suggests that the Jogan earthquake of A.D. 869 did not trigger the movement of the Itozawa fault at our trench site. Nevertheless, there are several other normal faults in southeast Fukushima, including the Yunodake fault and the eastern section of the Itozawa fault. It is still unknown whether these fault traces moved in association with the Jogan and/or possibly the historical 1611 Keicho earthquake, which both inundated the Sendai plain.

Discussion

Comparison to InSAR Analyses

InSAR analyses of the Iwaki earthquake, performed by GSI (2011) and Fukushima *et al.* (2012), exhibit two major, distinct traces of displacement discontinuity corresponding to the Itozawa and Yunodake fault ruptures we observed in the field. The interferogram fringe patterns clearly indicate that the fault sections had significant amounts of slip (Fig. 2 in Fukushima *et al.*, 2012). The Earth's surface west of the Itozawa fault and southwest of the Yunodake fault shows movement away from the satellite located west of the area on its ascending orbit and pointing downward and eastward. Such fringe patterns along both faults are consistent with normal fault movement. The maximum range increase (displacement away from the satellite) of 2.5 m was obtained near the center of the western strand of the Itozawa fault (Fukushima *et al.*, 2012). The line-of-sight (LOS) ground displacements were measured along the fringe discontinuities, which correspond to the surface rupture (Fig. 8). Locations of the two major fault ruptures and their slip distributions based on the InSAR analyses and our field survey are roughly the same. The maximum LOS offset values, corresponding to about 60% of the net slip, are 1.50 m and 0.85 m along the Itozawa and Yunodake faults, respectively (Fukushima *et al.*, 2012). The rupture ends detected in the interferograms, however, extend 1 to 4 km farther from the edges of our discernible rupture traces in the field. This may suggest that

Table 1
Calibrated Ages for Radiocarbon Samples Collected from Kakehashi Trench across the 2011 Itozawa Fault Rupture Zone

Sample Name	Radiocarbon Age	Unit	Wall	Material	δ 13 C(%)	Calibrated Age (2σ)		Laboratory Name
						Older Bound	Younger Bound	
KKH-S2	15,980 ± 50	100	South	Wood	−27.14 ± 0.42	19,400	18,910	IAAA-110975
KKH-S5	14,830 ± 40	90	South	Wood	−27.24 ± 0.41	18,510	17,740	IAAA-110976
KKH-S9	6,140 ± 30	20	South	Charcoal	−30.12 ± 0.30	7,160	6,950	IAAA-110977
KKH-N18	7,070 ± 30	20	North	Charcoal	−26.65 ± 0.32	7,960	7,850	IAAA-110980
KKH-N20	10,860 ± 30	40–50	North	Charcoal	−24.15 ± 0.30	12,890	12,620	IAAA-110981
KKH-N21	14,010 ± 40	90	North	Wood	−25.05 ± 0.34	17,410	16,820	IAAA-110982
KKH-N22	15,440 ± 40	120	North	Wood	−26.38 ± 0.44	18,820	18,550	IAAA-110983

displacements of less than ~10 cm cannot be identified in the field, particularly in areas without any cultural features.

Furthermore, the InSAR image revealed complex ruptures involving additional minor surface breaks (Fig. 2 in Fukushima *et al.*, 2012) that were missed by the field survey, which was limited by accessibility in the mountains and visibility of tiny offsets without cultural features. The eastern strand of the Itozawa fault and a NW-trending clear strand 0.5–1.5 km west of the Yunodake rupture, in particular, are visible in the InSAR image, which allows us to infer that the rupture process was complex, possibly producing shallower branches (Fukushima *et al.*, 2012). After the InSAR image was rendered, we used the fringe map to confirm several minor en echelon cracks and a small amount of warping of the rice paddies along the eastern trace of the Itozawa fault (*x* marks in Fig. 6). Despite the InSAR advantage of a detailed two-dimensional deformation image, we believe direct measurement in the field is still important for constraining the fault displacement, surface dip of the fault, and rake of the slip. Field work also complements the data recovered from the interferograms, for example, the center of the Itozawa fault that Fukushima *et al.* (2012) missed.

Simultaneous Rupture of the Itozawa and Yunodake Faults

Complex, simultaneous rupture of multiple subparallel normal faults is rare among similar shallow events around the globe. One could raise questions about this uncommon case. Did these two main ruptures of the Itozawa and Yunodake faults both occur during the Iwaki earthquake? Was there any distinguishable time gap between the two ruptures? There were also several $M \sim 6$ shocks before the Iwaki earthquake, which may cast some doubt on the contemporaneousness of the two surface ruptures.

During our field survey, we interviewed several local residents who lived near the faults. Because the earthquake occurred on a rainy late evening, most of the residents did not directly observe the emergence of the surface rupture on 11 April. They first identified ground breaks in the early morning of 12 April, which suggests that the fresh ruptures and scarps were a product of the Iwaki earthquake and not associated with either its predecessors or successors (aftershocks; an M_j 5.6 earthquake occurred 3.5 h after the mainshock, but the seismic moment of the M_j 5.6 earthquake is incomparable with the one inferred from the Yunodake fault rupture). The teleseismic moment release function of the Iwaki earthquake possibly separated into two peaks during the ~10-s rupture, but the peaks cannot be associated with the individual fault ruptures (Yamanaka, 2011). The large non-double-couple component in fault-plane solutions (U.S. Geological Survey, 2011) is consistent with the simultaneous rupture of the Itozawa and Yunodake faults acting to perturb the double-coupled moment tensor. Even though one fault might have been triggered by the other fault, there could be an indiscernible time gap between the two events. Because the hypocenter of the Iwaki earthquake is located ~3 km west of the southern edge of the Itozawa fault rupture, we suppose that the rupture commenced from the southern tip of the Itozawa fault and triggered the movement of the Yunodake fault during the ongoing rupturing of the Itozawa fault.

Furthermore, an InSAR-derived fault model (Fukushima *et al.*, 2012) suggests that the optimum dip angles for the Itozawa and Yunodake faults are 73° and 62°, which is in agreement with our field data and does not require a deeper connection of the two faults. The Iwaki earthquake occurred during the elevated seismicity influenced by the 11 March Tohoku mainshock. The computed Coulomb stress change (Toda *et al.*, 2011) of the NW-striking normal faults due to the M 9 event shows increased stress of up to ~15 bars in the Iwaki epicentral region, which corresponds roughly to one-third of a typical earthquake stress drop. We thus believe that heightened Coulomb (and/or shear) stress was so extensive as to promote normal faulting on all of the faults in the southern Abukuma highland region, the condition of which might contribute to producing not only swarmlike activity but also multiple and complex dynamic (or quasistatic) ruptures during the Iwaki earthquake.

Comparison with the Pichilemu Doublet Triggered by the 2010 Maule, Chile, Earthquake

Shallow normal faulting activity in the overriding plate triggered by an $M \sim 9$ megathrust earthquake is not unique to the Tohoku-oki earthquake. The M_w 8.8 Maule, Chile, earthquake that occurred on 27 February 2010 triggered similar normal faulting events near the northern end of the Maule rupture zone. A pair of large, shallow crustal earthquakes, M_w 6.9 and M_w 7.0, occurred within 15 min of each other near the town of Pichilemu on 11 March 2010 (Farias *et al.*, 2011; Ryder *et al.*, 2012). Numerous similarities exist between the Iwaki and Pichilemu cases: (1) Both earthquakes occurred in the forearc coastal region where inland active faults are sparsely distributed. (2) The stress field might have changed from weak compression to strong extension promoting normal faults closer to failure by more than 10 bars (up to 40 bars). (3) These large events occurred in a swarmlike, highly activated cluster triggered near the end of the megathrust rupture zone. (4) Both cases involved multiple ruptures, with a 15-min gap for the Pichilemu case. One significant difference of the Pichilemu case compared to the Iwaki is that neither distinctive coseismic surface rupture nor an active normal fault trace had been reported previously (Farias *et al.*, 2011; Ryder *et al.*, 2012). Another dissimilarity is that the Pichilemu normal faults extend to the interplate contact (Farias *et al.*, 2011), whereas the bottom of the Yunodake and Itozawa faults are evidently much shallower than the 50-km-deep plate interface beneath Iwaki. This suggests that a connection to a plate interface is not a requisite trigger for such shallow normal-faulting earthquakes. In any case, these two recent striking examples suggest that shallow

forearc seismicity should not be excluded from seismic hazard analysis.

Recurrence Interval of Normal Faults and Relationship with Megathrust Events

As observed in Chile, postmegathrust, shallow, forearc normal faulting might be a common feature of subduction zones. The occurrence of a large normal-faulting earthquake in a forearc area may suggest significant stress change, thus helping date past megathrust earthquakes. Stress accumulation on normal faults in the study area is not guaranteed if one assumes persistent low compressional stress under observed strain rates on the order of 10^{-7} per year (or even less during the recent 100 years; Hashimoto, 1990; Sagiya, 2004). Even though local EW tensional axis of fault plane solutions were resolved from pre-Tohoku-oki earthquakes (Imanishi *et al.*, 2012), the regional seismicity rate was extremely low (Kato *et al.*, 2011), and neither thrust faulting nor normal faulting is encouraged during the interseismic period of the Hamadori region. In other words, interseismic stress loading on these normal faults is not comparable with the coseismic stress imparted by the $M \sim 9$ source. If this were the case, paleoseismic trenching across the Yunodake and Itozawa faults would reveal paleoseismicity of not only these faults but also the $M \sim 9$ class megathrust events along the plate interface, possibly including the historical 869 Jogan and 1611 Keicho earthquakes.

Our paleoseismic trench revealed that the interevent time between the 2011 and the penultimate earthquakes on the Itozawa fault is from 12,620 to 17,410 years, which might be more than 10 times longer than the "super-cycle" of the M 9 type earthquakes estimated from tsunami deposits (e.g., Sawai *et al.*, 2007). There is certainly no guarantee that all M 9 events share a large coseismic slip offshore from Fukushima that can be a driving force for EW stretching in the Hamadori region. Even assuming that the normal faulting activity is stimulated by every M 9 event, however, the amount of coseismic Coulomb stress increase is less than one-third or one-quarter of a typical stress drop for a large earthquake. Thus, the Yunodake and Itozawa faults might have ruptured only once in several M 9 megathrust earthquakes. More active faults have been mapped in and around the Hamadori region. (Research Group for Active Faults in Japan, 1991; Nakata and Imaizumi, 2002; and others). If all faults were sufficiently excavated, most of the M 9 occurrences would be implicitly recovered.

Conclusions

We mapped and measured offsets along two ~15-km-long surface rupture zones produced by the 11 April 2011 Iwaki earthquake (M_w 6.6), which occurred a month after the M_w 9.0 Tohoku-oki, Japan, earthquake. These surface breaks occurred along previously mapped active fault traces, the Yunodake fault and Itozawa fault, both of which are reactivated normal faults of half-graben structures developed during the Tertiary Period. Interviews of local residents together with seismological data reveal that the two subparallel faults ruptured simultaneously. The maximum vertical displacement on the Yunodake fault is ~0.8 m, whereas that on the Itozawa fault is ~2.1 m. Even though we could not find surface breaks < 10 cm in the field, the location and slip distribution of the two major rupture zones are similar to those detected by InSAR analyses. Tectonic geomorphic features interpreted from aerial photos and the 2011 rupture along the Itozawa fault are characterized by uphill-facing scarps, in opposite sense to the large-scale topography. Rupture along the Yunodake fault occurred along a geologic fault juxtaposing Mesozoic metamorphic rocks against Neogene sedimentary rocks, exposing its high-angle bedrock fault. Based on hypocenter location, we interpret that the Itozawa fault moved first and then triggered normal faulting movement on the Yunodake fault under the heightened coseismic and postseismic Coulomb (and/or shear) stress due to the 11 March 2011 Tohoku-oki earthquake. A similar doublet of shallow crustal earthquakes was observed at Pichilemu after the 2010 M_w 8.8 Chile earthquake, which may suggest that the combination of M 9-class megathrust events and shallow forearc normal-faulting earthquakes is not unique to Tohoku but rather common. Nevertheless, our trench excavation across the 2011 rupture on the Itozawa fault did not expose any evidence of rupturing associated with the A.D. 869 Jogan earthquake, which is believed to be the penultimate M 9 earthquake and which widely inundated the Sendai plain. We instead found evidence of a surface-deforming earthquake that occurred sometime between 12,620 and 17,410 yr B.P. This does not mean that the recurrence interval of M 9 megathrust earthquakes is about 10,000 years. We rather believe that the Yunodake and Itozawa faults might have ruptured once in several M 9 megathrust earthquakes. More active faults have been mapped in and around the 2011 epicentral region. If all of these faults were sufficiently excavated, most of the M 9 occurrences might be implicitly recovered.

Data and Resources

All of the field data used in this paper are observations made by the authors. Epicentral locations and focal mechanisms were from the Japan Meteorological Agency (JMA) and the National Research Institute for Earth Science and Disaster Prevention (NIED), respectively. The geological map of the study area is provided by the Geological Survey of Japan, AIST (available at http://iggis1.muse.aist.go.jp/seamless/en/top.htm, last accessed April 2012). National Seismic Hazard Maps for Japan and associated evaluation reports can be seen at http://www.jishin.go.jp/main/w_hyoka-e.htm (last accessed April 2012, updated after the Tohoku-oki earthquake). Teleseismic information and teleseismic inversion of the Iwaki earthquake are available at http://earthquake.usgs.gov/earthquakes/eqinthenews/2011/usc0002n9v/ and http://www.seis.nagoya-u.ac.jp/sanchu/

Seismo_Note/2011/NGY38.html (last accessed December 2012). Topographic maps, a digital elevation model, and aerial photos were provided by Geospatial Information Authority of Japan (GSI). The OxCal program, developed by Bronk-Ramsey, is available for online use or downloadable at http://c14.arch.ox.ac.uk/oxcal.html (last accessed December 2012) to calibrate radiocarbon dates. Several figures were produced using Generic Mapping Tools available at http://gmt.soest.hawaii.edu (last accessed December 2012).

Acknowledgments

We thank Hirotake Yasuda, Nobuhiko Sugito, Masashi Omata, Yorihide Kohriya, Yoshiki Mori, Tatsuya Sugiyama, Daisuke Ishimura, and Shiho Hirose for their support during the field mapping and trench excavation study. We also thank Go Sato for providing us with his aerial photographs. Yo Fukushima, Manabu Hashimoto, Yoichiro Takada, Tomokazu Kobayashi, and Mikio Tobita generously shared the results of their InSAR analyses, which were valuable for surface rupture mapping. Our study was supported by a special emergency grant for the Tohoku-oki earthquake from the Disaster Prevention Research Institute, Kyoto University, and an international research project for the Tohoku-oki earthquake (J-RAPID) by the Japan Science and Technology Agency (JST).

References

Anan, S., S. Shinagawa, K. Yasumoto, Y. Wakisaka, and T. Eguchi (2011). Surface rupture associated with a large aftershock (April 11) of the Tohoku-oki earthquake, an initial report, http://www.pwri.go.jp/jpn/news/2011/0313/img/yoshin.pdf (last accessed December 2012, in Japanese).

Asano, Y., T. Saito, Y. Ito, K. Shiomi, H. Hirose, T. Matsumoto, S. Aoi, S. Hori, and S. Sekiguchi (2011). Spatial distribution and focal mechanisms of aftershocks of the 2011 off the Pacific coast of Tohoku Earthquake, *Earth Planets Space* **63,** 669–673.

DeMets, C., R. G. Gordon, and D. F. Argus (2010). Geologically current plate motions, *Geophys. J. Int.* **181,** 1–80, doi: 10.1111/j.1365-246X.2009.04491.x.

Farias, M., D. Comte, S. Roecker, D. Carrizo, and M. Pardo (2011). Crustal extentional faulting triggered by the 2010 Chilean earthquake: the Pichilemu seismic sequence, *Tectonics* **30,** TC6010, doi: 10.1029/2011TC002888.

Fukushima, Y., Y. Takada, and M. Hashimoto (2012). Complex Ruptures of the 11 April 2011 M_w 6.6 Iwaki Earthquake Triggered by the 11 March 2011 M_w 9.0 Tohoku Earthquake, Japan, *Bull. Seism. Soc. Am.* **103,** no. 2B, doi: 10.1785/0120120140.

Geospatial Information Authority of Japan (GSI) (2011). Fukushima Hamadori, Japan earthquake (M 7.0): crustal deformation detected by ALOS/PALSAR data, http://www.gsi.go.jp/cais/topic110425-index-e.html (last accessed December 2012).

Hasegawa, A., K. Yoshida, and T. Okada (2011). Nearly complete stress drop in the 2011 M_w 9.0 off the Pacific coast of Tohoku Earthquake, *Earth Planets Space* **63,** 703–707, doi: 10.5047/eps.2011.06.007.

Hashimoto, M. (1990). Horizontal strain rates in the Japanese Islands during interseismic period deduced from geodetic surveys (Part I): Honshu, Shikoku and Kyushu, *Zisin* **43,** 13–26 (in Japanese with English abstract and captions).

Headquarters for Earthquake Research Promotion (2011). Long-term earthquake probabilities on subduction zones and major active faults, Earthquake Research Committee, Headquarters for Earthquake Research Promotion, available from http://www.jishin.go.jp/main/choukihyoka/ichiran_past/ichiran20110111.pdf (last accessed December 2012, in Japanese).

Ide, S. (2011). Shallow dynamic overshoot and energetic deep rupture in the 2011 M_w 9.0 Tohoku-Oki earthquake, *Science* **332,** 1426–1429, doi: 10.1126/science.1207020.

Imamura, F., and S. Anawat (2012). Damage due to the 2011 Tohoku earthquake tsunami and its lessons for future mitigation, in *Proc. of the International Symposium on Engineering: Lessons Learned from the 2011 Great East Japan Earthquake*, 21–30.

Imanishi, K., R. Ando, and Y. Kuwahara (2012). Unusual shallow normal-faulting earthquake sequence in compressional northeast Japan activated after the 2011 off the Pacific coast of Tohoku earthquake, *Geophys. Res. Lett.* **39,** L09306, doi: 10.1029/2012GL051491.

Ishiyama, T., N. Sugito, T. Echigo, and H. Sato (2011). The surface earthquake fault of the 11 April 2011 earthquake in Hamadoori Fukushima pref., http://outreach.eri.u-tokyo.ac.jp/eqvolc/201103_tohoku/eng/hamadoori/#report1 (last accessed December 2012, in Japanese).

Kano, H., Y. Kuroda, K. Uruno, T. Mureki, S. Kanisawa, T. Maruyama, H. Umemura, H. Mitsukawa, N. Seto, Y. Ohira, S. Sato, and N. Issiki (1973). Geology of the Takanuki district, Geological Survey of Japan, quadrangle series, scale 1:50,000, Niigata (7), No. 70. 109 p.

Kato, A., E. Kurashimo, N. Hirata, S. Sakai, T. Iwasaki, and T. Kanazawa (2005). Imaging the source region of the 2004 mid-Niigata prefecture earthquake and the evolution of a seismogenic thrust-related fold, *Geophys. Res. Lett.* **32,** L07307, doi: 10.1029/2005GL022366.

Kato, A., S. Sakai, and K. Obara (2011). A normal-faulting seismic sequence triggered by the 2011 off the Pacific coast of Tohoku Earthquake: wholesale stress regime changes in the upper plate, *Earth Planets Space* **63,** 745–748, doi: 10.5047/eps.2011.06.014.

Kurosawa, H., F. Sato, and A. Miwa (2011). A survey report on surface rupture along the Itozawa fault, http://www.oyoene-db.com/web/topics_h_001.html (last accessed December 2012, in Japanese).

Lin, A., S. Toda, G. Rao, S. Tsuchihashi, and B. Yan (2012). Structural analysis of coseismic normal fault zones of the 2011 M_w 6.6 Fukushima earthquake, Northeast Japan, *Bull. Seism. Soc. Am.* **103,** no. 2B, doi: 10.1785/0120120111.

Mitsui, S. (1971). Studies on the mechanism of deformation of sedimentary rocks in the Iwaki area of the Joban coal-field, Fukushima Prefecture, *Tohoku Univ., Sci. Report*, 2nd, series (Geol.), **42**, 199–272.

Mori, N., T. Takahashi, T. Yasuda, and H. Yanagisawa (2011). Survey of 2011 Tohoku earthquake tsunami innundation and run-up, *Geophys. Res. Lett.* **38,** L00G14, doi: 10.1029/2011GL049210.

Nakata, T. and T. Imaizumi, eds. (2002). *Digital Active Fault Map of Japan*, Univ. Tokyo Press, Tokyo, DVD and 66 p.

Nohara, T., Y. Koriya, and T. Imaizumi (2000). An estimation of the crustal strain rate using the active fault GIS data, *Active Fault Res.* **19,** 23–32 (in Japanese with English abstract).

Okamura, Y., K. Satake, K. Ikehara, A. Takeuchi, and K. Arai (2005). Paleoseismology of deep-sea faults based on marine surveys of northern Okushiri ridge in the Japan Sea, *J. Geophys. Res.* **110,** B09105, doi: 10.1029/2004JB003135.

Ozawa, S., T. Nishimura, H. Suito, T. Kobayashi, M. Tobita, and T. Imakiire (2011). Coseismic and postseismic slip of the 2011 magnitude-9 Tohoku-Oki earthquake, *Nature* **475,** 373–376, doi: 10.1038/nature10227.

Reimer, P. J., M. G. L. Baillie, E. Bard, A. Bayliss, J. W. Beck, P. G. Blackwell, C. Bronk-Ramsey, C. E. Buck, G. S. Burr, R. L. Edwards, M. Friedrich, P. M. Grootes, T. P. Guilderson, I. Hajdas, T. J. Heaton, A. G. Hogg, K. A. Hughen, K. F. Kaiser, B. Kromer, F. G. McCormac, S. W. Manning, R. W. Reimer, W. Ron, D. A. Richards, J. R. Southon, S. Talamo, C. S. Turney, J. van der Plicht, and C. E. Weyhenmeyer (2009). IntCal09 and Marine09 radiocarbon age calibration curves, 0-50,000 years cal BP, *Radiocarbon* **51,** 1111–1150.

Research Group for Active Faults in Japan (1991). *Active Faults in Japan, Sheet maps and Inventories*, Revised Ed., Univ. Tokyo Press, Tokyo, 437 p.

Ryder, I., A. Rietbrock, K. Kelson, R. Burgmann, M. Floyd, A. Socquet, C. Vigny, and D. Carrizo (2012). Large extensional aftershocks in the continental forearc triggered by the 2010 Maule earthquake, Chile, *Geophys. J. Int.* **188,** 879–890, doi: 10.1111/j.1365-246X.2011.05321.x.

Sagiya, T. (2004). A decade of GEONET: 1994-2003: the continuous GPS observation in Japan and its impact on earthquake studies, *Earth Planet Space* **56,** 29–41.

Sato, H. (1994). The relationship between late Cenozoic tectonic events and stress field and basin development in northeast Japan, *J. Geophys. Res.* **99,** no. B11, doi: 10.1029/94JB00854.

Sato, H., S. Kawasaki, S. Abe, N. Kato, T. Iwasaki, and T. Ito (2007). Seismic reflection profiling across the onshore source area of the 2007 Noto Hanto earthquake, central Japan, *Bull. Earthq. Res. Inst. Univ. Tokyo* **82,** 265–273 (in Japanese with English abstract and captions).

Sawai, Y., M. Shishikura, Y. Okamura, K. Takada, T. Matsu'ura, T. T. Aung, J. Komatsubara, Y. Fujii, O. Fukuwara, K. Satake, T. Kamataki, and N. Sato (2007). A study on paleotsunami using handy geoslicer in Sendai Plain (Sendai, Natori, Iwanuma, Watari, and Yamamoto), *Miyagi, Japan, Annual Report on Active Fault and Paleoearthquake Researches* **7,** 47–80 (in Japanese with English abstract and captions).

Sieh, K., D. H. Natawidjaja, A. J. Meltzner, C.-C. Shen, H. Cheng, K. S. Li, B. W. Suwargadi, J. Galetzka, B. Philibosian, and R. L. Edwards (2008). Earthquake supercycles inferred from sea-level changes recorded in the corals of west Sumatra, *Science* **322,** 1674–1678, doi: 10.1126/science.1163589.

Simons, M., S. E. Minson, A. Sladen, F. Ortega, J. Jiang, S. E. Owen, L. Meng, J.-P. Ampuero, S. Wei, R. Chu, D. V. Helmberger, H. Kanamori, E. Hetland, A. W. Moore, and F. H. Webb (2011). The 2011 magnitude 9.0 Tohoku-Oki earthquake: Mosaicking the megathrust from seconds to centuries, *Science* **332,** 1421–1425.

Suwa, Y., S. Miura, A. Hasegawa, T. Sato, and K. Tachibana (2006). Interplate coupling beneath NE Japan inferred from three-dimensional displacement field, *J. Geophys. Res.* **111,** B04402, doi: 10.1029/2004JB003203.

Toda, S., R. S. Stein, and J. Lin (2011). Widespread seismicity excitation throughout central Japan following the 2011 $M = 9.0$ Tohoku earthquake and its interpretation by Coulomb stress transfer, *Geophys. Res. Lett.* **38,** L00G03, doi: 10.1029/2011GL047834.

U.S. Geological Survey (USGS) (2011). USGS centroid moment solution, magnitude 7.1 eastern Honshu, Japan, http://earthquake.usgs.gov/earthquakes/eqinthenews/2011/usc0002n9v/neic_c0002n9v_cmt.php (last accessed December 2012).

Wesnousky, S. G., C. H. Scholz, and K. Shimazaki (1982). Deformation of an island arc: rates of moment release and crustal shortening in intraplate Japan determined from seismicity and Quaternary fault data, *J. Geophys. Res.* **87,** 6829–6852.

Yamanaka, Y. (2011) Source model of the April 11, 2011, Fukushima-Hamadori earthquake (M 7.0) analysed with teleseismic body waves, http://www.seis.nagoya-u.ac.jp/sanchu/Seismo_Note/2011/NGY38.html (last accessed April 2012, in Japanese).

International Research Institute of Disaster Science (IRIDeS)
Tohoku University
Aoba, 6-6, Aramaki, Aoba-ku
Sendai 980-8578, Japan
toda@irides.tohoku.ac.jp
(S.T.)

Department of Geophysics, Graduate School of Science
Kyoto University
Kitashirakawa-oiwake-cho, Sakyo-ku
Kyoto 606-8502, Japan
tsutsumh@kugi.kyoto-u.ac.jp
(H.T.)

Manuscript received 18 September 2012